XAFS Study of U(VI) Bioremediation Products

S. D. Kelly,[1] K. M. Kemner,[1] Y. Suzuki,[2] J. F. Banfield[2,3]
[1]Argonne National Laboratory, Argonne, IL, U.S.A.
[2]University of Wisconsin-Madison, WI, U.S.A.
[3]*Present address: University of California, Berkeley, CA, U.S.A.*

Introduction

Contamination of sediments and water by actinides, including U, is a serious international problem. The discovery that bacteria can convert mobile uranyl carbonate ions to uraninite (UO_2) spurred the development of strategies for *in situ* bioremediation of uranium-contaminated lands. These approaches are based on the extremely low solubility of uraninite (K_{sp} ~10^{-61}). Although the products of biological actinide reduction are known to be amorphous or poorly crystalline, their detailed structure, form, and reactivity and the implications of these characteristics for uranium mobility have not been completely determined. We show that biogenic uraninite particles are almost as small as crystals can be. This small particle size might make uraninite much more mobile than previously thought, because of particulate transport. Therefore, bioremediation strategies based on the formation of uraninite might not diminish the transport of uranium in the subsurface.

Methods and Materials

We examined the uraninite that formed when complex natural-uranium-contaminated sediments were incubated with an organic substrate designed to stimulate growth of native anaerobic bacteria. X-ray absorption fine structure (XAFS) measurements were made on samples (P3) held in a Teflon® sample holder and sealed between two pieces of Kapton® film to maintain anaerobic conditions. We also measured a uraninite standard diluted 1:100 with SiO_2 in fluorescence mode. All XAFS measurements were made at the Materials Research Collaborative Access Team (MR-CAT) beamline at the APS [1]. The energy of the incident x-rays was selected by using a Si(111) monochromator. Higher harmonics were rejected by using reflection from a Rh mirror. The incident x-ray intensity was sampled with a nitrogen-filled ion chamber, and the fluorescent x-ray intensity was sampled with an Ar-filled fluorescence detector in the Stern-Heald geometry [2]. A Sr filter of three absorption lengths was used to reduce the background signal. Linearity tests [3] indicated less than 0.30% nonlinearity for a 50% decrease in incident x-ray intensity. The incident x-ray intensity varied by less than 15% throughout the energy range of the XAFS measurements.

The sample was exposed to the x-ray beam for approximately 1 min for each of the measurements. Measuring several spectra at different sample locations enabled determination of radiation-induced chemical effects at the 1-min timescale. No time-dependent change in the XAFS data was observed for any of the samples. X-ray absorption near-edge structure (XANES) data were normalized by using standard procedures. The transmission XAFS signal of a Y foil, as described elsewhere [4], was used as a reference to accurately align the edge-energy positions of the U(IV) (UO_2) and U(VI) (UO_3) standards and the P3 data. In all, 30-50 scans from six different locations on each sample were averaged.

The codes contained in the University of Wisconsin UWXAFS package [5] were used to analyze the data. The program FEFF7 [6] was used to construct the theoretical model on the basis of the crystallographic atomic position of uraninite [7]. The theoretical models are built from scattering paths of the photoelectron. The error analysis and the goodness-of-fit parameters were calculated with the fitting routine FEFFIT. The structural parameters determined in a fit to the XAFS data include N_{degen} and R, which are the number of neighboring atoms and the distance to them for a single scattering path, respectively, and σ^2, which is the relative mean square displacement of the absorbing U atom and the neighboring atoms for a single scattering path.

The data range (k = 2.0-10.0 and 3.0-11.5 $Å^{-1}$), fit range (R = 1.0-4.3 and 1.0-4.2 Å), and a Fourier transform Hanning window with a sill width (dk) of 1.0 $Å^{-1}$ and k-weightings of 1, 2, and 3 were used in the analysis of the P3 and UO_2 data, respectively. S_0^2 was determined to be 0.9 ±0.1 from the UO_2 data. ΔE_0 was determined to be 2.0 ±1.2 and –2.1 ±0.5 for all paths of the UO_2 and P3 data, respectively. For the axial oxygen shell, σ^2 was constrained to 0.002 $Å^2$, as determined previously [8].

Results

The theoretical model is based on the crystal structure of UO_2 and generated by FEFF7. The UO_2 data were modeled first to determine the important scattering paths of the photoelectron. Paths from the first two oxygen shells and the first uranium shell, plus the multiple scattering paths from two oxygen atoms in the first shell, contributed significantly to the XAFS data (Table 1). Table 1 lists the best-fit results. This model was applied to the P3 data. Inclusion of additional Oax, C, and O paths at ~1.8, 2.9, and 3.8 Å, respectively, was required to

Table 1. Best-fit values for the UO_2 and P3 sample.

Path	N_{degen}	R (Å)	σ^2 (10^{-3} Å^2)
UO_2 sample			
U-O1	8.0	2.35±0.01	9±2
U-U	11.7±4.0	3.87±0.01	5±2
U-O2	23.3±8.0	4.49±0.02	9±3
U-O1-O1	8.0	4.70±0.03	19±4
U-O1-U-O1	8.0	4.70±0.03	19±4
U-O1-U-O2	8.0	4.65±0.04	19±4
P3 sample			
U-Oax	0.5±0.1	1.77±0.01	2
U-O1	7.4±1.0	2.34±0.01	12±1
U-C	2.6±0.8	2.92±0.01	1±4
U-Oax1-U-Oax1	0.9±0.1	3.54±0.02	4
U-Oax1-Oax2	0.9±0.1	3.54±0.02	4
U-Oax1-U-Oax2	0.9±0.1	3.54±0.02	4
U-O2	7.0±5.7	3.85±0.05	19±15
U-U	5.6±4.0	3.80±0.02	19±10

decrease the R-factor from an unsatisfactory 9% to 0.5%. The data and best-fit model are shown in Fig. 1. The presence of the Oax signal indicates that some of the uranium was not reduced. Our fit results (Table 1) indicate ~0.5 Oax atoms, corresponding to ~25% U^{6+} in this sample. The U-to-C distance of 2.92 Å (Table 1) indicates that the carbon atom forms a strong bidentate complex with U [8]. The U-to-O distance of 3.85 Å (Table 1) is consistent with a water molecule that is ~2.5 Å above the oxygen-terminated surface of the uraninite structure — an additional ~1.35 Å from the U atom — as was seen previously [9].

Discussion

The XANES results confirmed that most of the uranium in the P3 sediment was reduced to U^{4+} (Fig. 2). The EXAFS results confirm that uraninite particles are small because of the low coordination number for the number of U-U neighbors (5.6 ±4.0). The average uraninite particle is 1.8 to 1.3 nm in diameter, on the basis of 5.6 neighbors, with 4 to 5 U-U neighbors on the surface of the uraninite particle. The large uncertainty in the number of U-U neighbors indicates the potential for as many as 9.6 U-U neighbors, consistent with a particle diameter of 6.8 to 2.9 nm with 4 to 8 U-U neighbors on the surface of the particle. Therefore, the range of possible particle diameters, on the basis of an extended XAFS (EXAFS) U-U coordination number, ranges from 1.3 to 6.8 nm. The formation of uraninite nanoparticles is significant, because the mobility of U in the subsurface could be based on particulate transport rather than the extremely low solubility of uraninite.

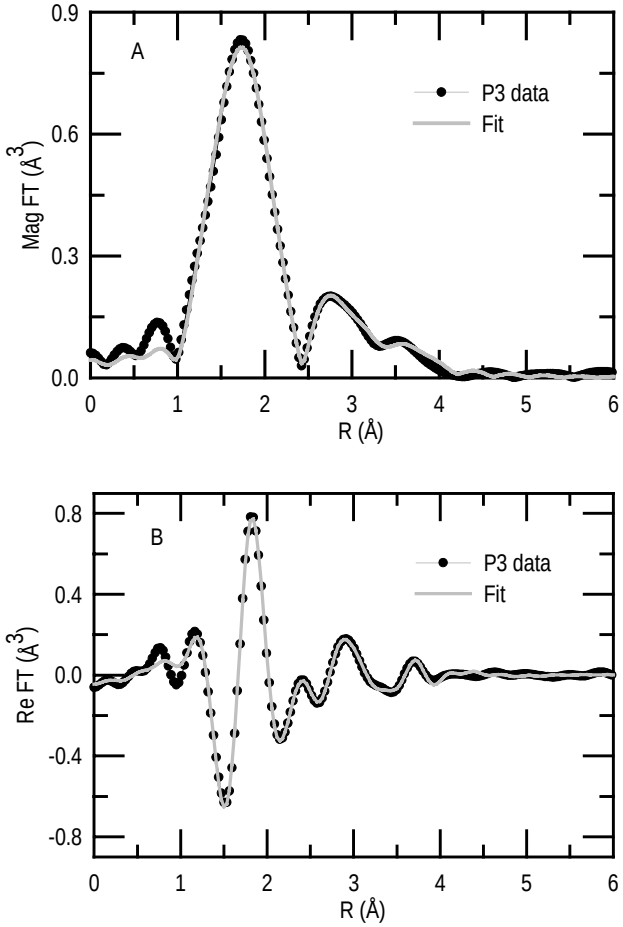

FIG. 1. The (a) magnitude and (b) real part of the Fourier transform of the best-fit model, with data from the P3 sample.

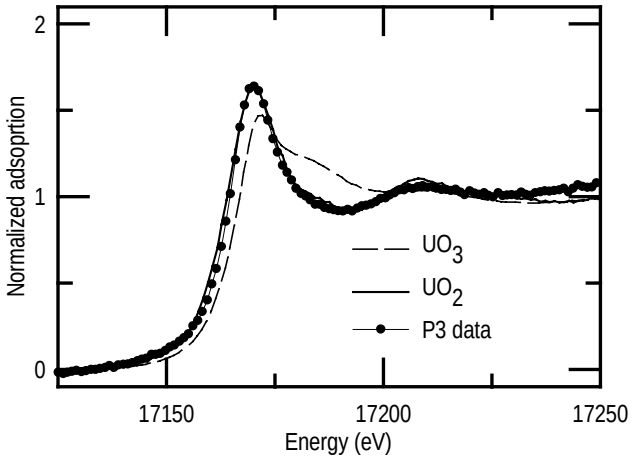

FIG. 2. Average normalized absorption data from UO_2, UO_3, and the P3 sample.

Acknowledgments

This work was supported by the U.S. Department of Energy (DOE), Office of Biological and Environmental Research, Natural and Accelerated Research (NABIR) program. MR-CAT is supported by DOE under Contract No. DE-FG02-94-ER45525 and by the member institutions. Use of the APS was supported by the DOE Office of Science, Office of Basic Energy Sciences, under Contract No. W-31-109-ENG-38.

References

[1] C. U. Segre, N. E. Leyarovska, and L. D. Chapman et al., in *Synchrotron Radiation Instrumentation: Eleventh U.S. Conference*, CP521, 419-422 (2000).

[2] E. A. Stern and S. M. Heald, Rev. Sci. Instrum. **50**, 1579-1583 (1979).

[3] K. M. Kemner, A. J. Kropf, and B. A. Bunker, Rev. Sci. Instrum. **65**, 3667-3669 (1994).

[4] J. L. Cross and A. I. Frenkel, Rev. Sci. Instrum. **70**, 38-40 (1998).

[5] E. A. Stern, M. Newville, and B. Ravel et al., Physica B **208** and **209**, 2995-3009 (1995).

[6] S. I. Zabinsky, J. J. Rehr, and A. Ankudinov et al., Phys. Rev. B **52**(4), 2995-3009 (1995).

[7] R. W. G. Wyckoff, *Crystal Structures* (Interscience Publishers, New York, NY, 1960).

[8] P. G. Allen, J. J. Bucher, and D. L. Clark et al., Inorg. Chem. **34**, 4797-4807 (1995).

[9] L. Cheng, P. Fenter, and K. L. Nagy et al., Phys. Rev. Lett. **87** (15) (2001).